Journal of Physical and Theoretical Chemistry
of Islamic Azad University of Iran, 4 (4) 197-203**:** Winter 2008
(J.Phys.Theor.Chem.IAU Iran: Winter 2008)
ISSN: 1735-2126

Sensing of Methanol and Ethanol with Nano-Structured SnO_2 (110) in Gas Phase: Monte Carlo Simulation

N. Mangkorntong[1], L. Mahdavian[2], F. Mollaamin[3] and M. Monajjemi[4*]

1. Department of Physics, Faculty of Science, Chiang Mai University, Chiang Mai, Thailand
2. Department of Chemistry, Doroud Branch, Islamic Azad University, Doroud, Iran, P.O. Box: 133.
3. Department of Chemistry, Qom Branch, Islamic Azad University, Qom, Iran
4. Department of Chemistry, Science & Research Branch, Islamic Azad University ,Tehran, Iran, P.O. Box: 14155-775

ABSTRACT

The SnO_2 films deposited from inorganic precursors via sol–gel dip coating method have been found to be highly sensitive to methanol and ethanol vapor. Three dimensional nano-structure materials have attracted the attention of many researches because the possibility to apply them for near future devices in sensors, catalysis and energy related. The sensitivity and selectivity of SnO_2 (110) nano-structure is calculated in interaction with different concentrations (25 wt. %, 50wt. % and 75 wt. %) of methanol and ethanol vapor. The energy of this interaction is investigated in different distances CH_3OH and C_2H_5OH vapor related to SnO_2 (110). The calculations achieved by methods of Monte Carlo simulation in different temperatures. All the calculations were carried out using Hyperchem 7.0 package of program. The total energy increased with addition blends of alcohol molecules and temperature so the interactions between them are endothermic. The excellent sensitivity and selectivity of SnO_2 is at 443K for blend of 75 wt.% them in 7 Å distances.

Keywords: Tin dioxide [SnO_2 (110)]; Methanol and Ethanol; RMS gradient; acceptance ratio (ACCR); Monte Carlo Simulation

INTRODUCTION

Ethanol is the most popular member of alcohol family because of a rare blend of its useful and harmful effects. This is the only alcohol which most of the people all over the world encounter to day life. Detection and control of ethanol is necessary for the well being of the society. Ethanol sensors find applications in various areas such as the control of drunken driving and the monitoring of fermentation and other processes in chemical industries.

Development of ethanol sensors based on thin film technology offers the advantages of greater sensitivity, shorter response time and lower costs. A variety of mature physical and chemical vapor deposition methods and their hybrids have in the past been used to deposit SnO_2 [1] the active layer of an ethanol sensor.
Tin dioxide is the most used material for gas sensing because its three - dimensional nanostructures and properties are related to the

* . Corresponding author:m_monajjemi@yahoo.com

large surface exposed to gas adsorption. It has been suggested that nanometer sized particles, properly prepared and treated, might be used to form the high surface area analogues of known catalysts or sensors to provide improved efficiency of existing catalytic or sensor function [2, 3]. In this paper, we used tin dioxide because present great potential properties for applications as optoelectronic devices, gas sensor, solar energy or even for detecting leakages of reducing gases such as H, H_2S, CO, methanol and ethanol [4].

The theoretical study of such surface adsorb interactions provides a valuable tool to get superior performances that are unattainable using only a trial-and-error approach together with a powerful analytic methodology to explain the experimental data [5].

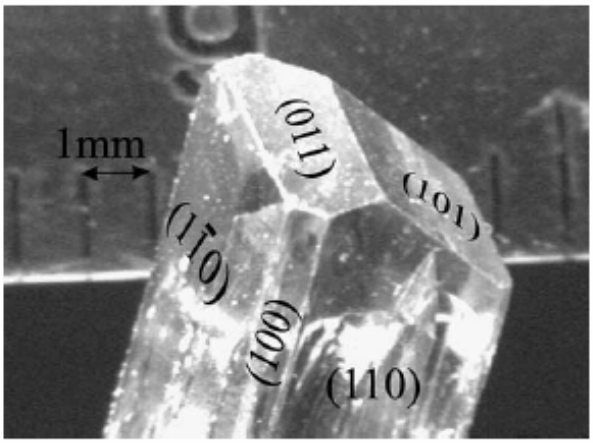

Fig.1. Photograph of a SnO_2 single crystal grown by a vapor phase transport technique [6].

For these bulk terminated SnO_2 surfaces, i.e. surfaces with surface-tin atoms in their bulk Sn^{4+} oxidation state, the (110) surface exhibits the lowest energy surface followed by the (100), (101), and (001) surfaces. The fact that the (110) surface is the lowest energy surface can be appreciated by investigating the crystallographic orientations of the bulk termination of single crystals [6]. A photograph of a single crystal grown by a vapor phase transport technique is shown in Fig. 1. It is obvious that the (110) surfaces make up the majority of the surface area followed by the (101) faces and small (100) faces. Representations of the bulk-terminated surfaces are shown in Fig. 2, left side panels. These surfaces are constructed in an auto compensated way, i.e. the same number of Sn-to-O as O-to-Sn bonds are cut. This is a rule that often allows assessing the most likely surface termination of ionic crystals [7]. Two single phonon losses were identified at 339 cm^{-1} and 694 cm^{-1}. In HREELS similar to IR spectroscopy only the A_2u and Eu modes are active because only these modes involve the necessary dipole change.

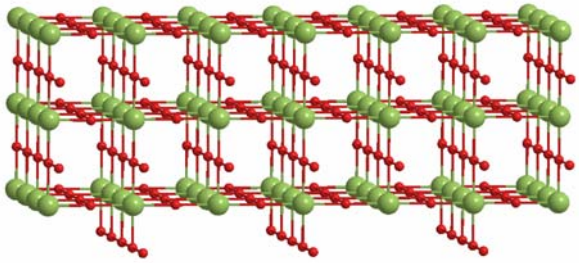

Fig.2. Ball-and-stick models of SnO_2 (110) low index surfaces. On the left-hand side stoichiometric bulk terminations are represented. This surface was obtained by removing twofold coordinated bridging oxygen rows from the stoichiometric surfaces.

Despite the importance of molecular interactions with SnO_2 in its applications as gas sensor and heterogeneous catalyst, relatively few surface science studies of molecular adsorption and reactions on SnO_2 single crystals have been performed. Furthermore, most of these studies have been concentrated on the SnO_2 (110) surface.

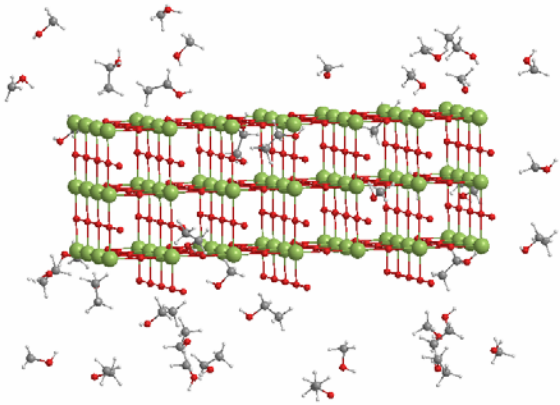

Fig.3. Interaction between SnO_2 (110) and methanol / ethanol (20/20 wt. %) molecules in mean of distance 7.0 A°.

In the present study, the aim of the present work is to provide theoretical hints for the development of improved CH_3OH and C_2H_5OH gas sensors using SnO_2 as the base sensing material that a pattern interaction between SnO_2 (110) and 40 molecules methanol/ethanol (20/20 wt.%) in mean distance 7.0 Å that is shown in Fig.3 and an attempt has been made to improve the selectivity and sensitivity of tin oxide-based these gases sensors along with lowering of operating temperature by decrease distance and adding wt.% methanol in gas phase. Interaction between them is investigated by using Monte Carlo simulation method with Hyperchem 7.0 program package [8].

CALCULATION DETAILS

The Metropolis implementation of the Monte Carlo algorithm has been developed by studying the equilibrium thermodynamics of many-body systems [9]. Especially for proteins of large size, the energy landscape is significantly more rugged than the energy landscape of small proteins [10. Therefore, the rank of native structure could be relatively better when ranked by the second force field [11]. In order to compute the average properties from a microscopic description of a real system, one shall evaluate integrals over phase space. It may be calculated for an *N*-particle system in an ensemble with distribution function $\boldsymbol{P}\ (r^N)$, the experimental value of a property $A\ (r^N)$ from:

$$\langle A(r^N)\rangle = \int A(r^N)P(r^N)dr^N \qquad (1)$$

The problem with direct evaluation of this multi-dimensional integral (apart of the huge number of phase space points as a sample) is that most of the configurations sampled contribute nothing to the integral. Having energy is so high that the probability of their occurrence is vanishingly small [12]. The RMS gradient that is reported is just the root-mean square average of the Cartesian components of the gradient vector.

For multi-dimensional potential energy surfaces a convenient measure of the gradient vector is the root-mean-square (RMS) gradient described by RMS Gradient:

$$(3N)^{-1}\left[\sum_A (\frac{\partial E}{\partial X_A})^2 + (\frac{\partial E}{\partial Y_A})^2 + (\frac{\partial E}{\partial Z_A})^2\right]^{1/2} \qquad (2)$$

For a molecular mechanics calculation the energy and the gradient are essentially the only quantities available from a single point calculation. In the case of MM^+, a much more complete description of the individual contributions to the energy, including individual stretch energies, bending energies, etc., is placed in the log file along with the system dipole moment, if bond dipoles are available.

The Monte Carlo Averages setup is identical to Molecular Dynamics Averages setup. There is an additional parameter that you can monitor in Monte Carlo: the acceptance ratio. It appears as ACCR on the list of possible selections in the Monte Carlo Averages dialog box; the RMS deviation of ACCR from its mean, appears also. The acceptance ratio is a running average of the ratio of the number of accepted moves to attempted moves. Optimal values are close to 0.5. Varying the step size can have a large effect on the acceptance ratio.

RESULTS AND DISCUSSION

Gas sensing calculations were performed at different temperatures in order to find out the optimum operating temperature of nano-structures of about 120 nm thick nesses of pure tin oxide in different blends methanol/ethanol (25 wt.%, 50 wt.% and 75wt%) were investigated for their structural and surface morphological properties. The sensitivity values these gases (40 molecules for all gases) for different wt. % are tabulated in tables.1-2.

Table 1. The total energy, kinetic energy, Sum Kinetic + potential energy, (kcal / mol), RMS gradient (kcal/mol·Å) and acceptance ratio (ACCR) calculated in distances (Å) by Monte Carlo simulation for SnO_2 (110) and different wt.% (methanol/ethanol) at 298 and 343K.

Distance (A)	25% (wt.% -Methanol/Ethanol)									
	298K					343K				
	E_{total}	ACCR	E_{kin}	$E_{(kin+pot)}$	RMS	E_{total}	ACCR	E_{kin}	$E_{(kin+pot)}$	RMS
4.00	243462.50	0.908	509.59	247031.07	709.90	243652.50	0.914	586.54	247197.74	703.00
7.00	248470.20	0.905	511.38	251282.02	727.30	248484.30	0.914	588.60	251427.62	750.50
10.00	248221.80	0.906	512.28	251863.72	742.60	248545.80	0.916	589.63	252171.13	742.00
12.00	249950.40	0.903	512.28	252523.42	732.30	250271.00	0.911	589.63	252741.37	740.60
Distance (A)	**50% (wt.% -Methanol/Ethanol)**									
4.00	243284.50	0.900	482.67	247184.13	687.30	243587.40	0.906	555.56	247355.63	673.50
7.00	247686.10	0.899	485.36	251818.74	701.00	247904.00	0.911	558.66	251931.91	714.00
10.00	248381.20	0.899	485.36	252522.42	720.70	248622.20	0.904	558.66	252672.40	724.60
12.00	249270.40	0.892	485.36	253456.46	733.30	249640.20	0.905	558.66	253713.66	708.90
Distance (A)	**75% (wt.% -Methanol/Ethanol)**									
4.00	243462.50	0.893	455.76	247402.37	709.90	243652.50	0.903	524.58	247527.66	703.00
7.00	248470.20	0.893	458.45	252523.01	727.30	248484.30	0.902	527.68	252574.47	750.50
10.00	248221.80	0.894	458.45	252409.88	742.60	248545.80	0.904	527.68	252617.06	742.00
12.00	249950.40	0.888	463.83	254182.51	732.30	250271.00	0.897	533.87	254376.08	740.60

Table 2. The total energy, kinetic energy, Sum Kinetic + potential energy, (kcal / mol), RMS gradient (kcal/mol·Å) and acceptance ratio (ACCR) calculated in distances (Å) by Monte Carlo simulation for SnO_2 (110) and different wt. % (methanol/ethanol) at 398 and 443K.

Distance (A)	25% (wt.%- Methanol/Ethanol)									
	398K					443K				
	E_{total}	ACCR	E_{kin}	$E_{(kin+pot)}$	RMS	E_{total}	ACCR	E_{kin}	$E_{(kin+pot)}$	RMS
4.00	244020.90	0.922	680.59	247479.77	686.00	244149.60	0.927	757.54	247648.17	705.00
7.00	248901.90	0.925	682.98	251669.81	733.70	249101.60	0.930	760.21	251883.41	731.70
10.00	248814.60	0.923	684.18	252226.02	742.90	249173.10	0.926	761.54	252462.64	742.80
12.00	250571.70	0.920	684.18	252961.82	725.20	250743.00	0.925	761.54	253070.19	750.70
Distance (A)	**50% (wt.% -Methanol/Ethanol)**									
4.00	243658.60	0.917	644.64	247440.78	684.10	244074.70	0.925	717.53	247642.25	672.30
7.00	248199.90	0.919	648.24	252127.34	715.80	248422.80	0.923	721.53	252282.39	720.10
10.00	248919.80	0.915	648.24	252878.02	718.10	249288.20	0.923	721.53	253092.50	698.60
12.00	249823.00	0.913	648.24	253833.68	723.20	250315.70	0.919	721.53	254121.42	705.00
Distance (A)	**75% (wt.% -Methanol/Ethanol)**									
4.00	244020.90	0.911	608.69	247725.57	686.00	244179.50	0.909	670.81	245349.45	705.40
7.00	248901.90	0.912	612.29	252841.49	733.70	259101.60	0.919	681.52	252985.33	731.70
10.00	248814.60	0.913	612.29	252817.20	741.90	249173.10	0.920	681.52	253011.93	742.80
12.00	250571.70	0.910	619.48	254568.66	725.20	250743.00	0.915	689.52	254674.69	750.70

The prominent peak is corresponding to increasing weight percent (wt. %) methanol at 298, 343 and 398K that is depended to dielectric constant. No peak corresponding at 443K is observed. Fig.4 is shown that the lower energy is for 50% weight methanol at all temperatures.

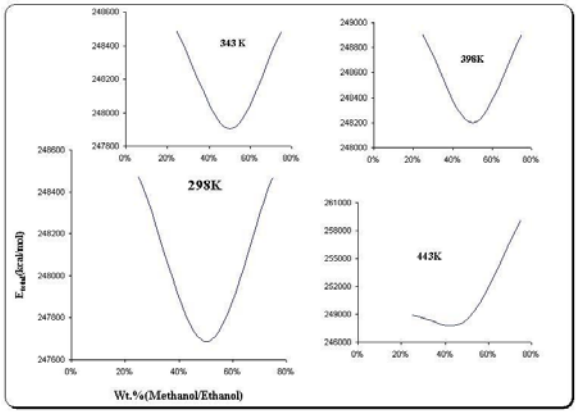

Fig.4. The total energy (kcal / mol) is calculated for interaction different wt. % methanol/ethanol with SnO_2 in distance (7.0 Å) at different temperatures by Monte Carlo simulation.

The tin oxide (SnO_2) is a well-known n-type semiconducting oxide that has been widely used for reducing gases in an operating temperature range of 273–443 K. This oxide material has high reactivity towards reducing gases at relatively low operating temperature, easy adsorption of oxygen on its surface because of its natural non-stoichiometry, stable phase and many more desirable attributes such as cheapness and simplicity. In spite of this, very few attempts have been made to develop nano-structures SnO_2 sensors operating at low temperature Fig.5.

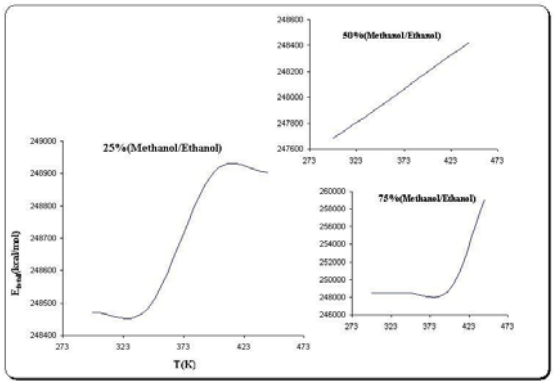

Fig.5. The total energy (kcal / mol) is calculated for interaction SnO_2 with different wt.% methanol /ethanol at different temperatures in distance (7.0 Å) by Monte Carlo simulation.

The total energy is calculated for interaction SnO_2 nano-structure and blends CH_3OH/C_2H_5OH vapor molecules in different distances in tables. 1-2. In lower distances, sensitivity and selectivity of SnO_2 is increased that with adding distance, its sensitivity reduces. But in relation to 75% of methanol/ethanol blend in Fig.6, A peak in 7.0 Å of distance is observed that numbers of methanol molecular play important role in this interaction.

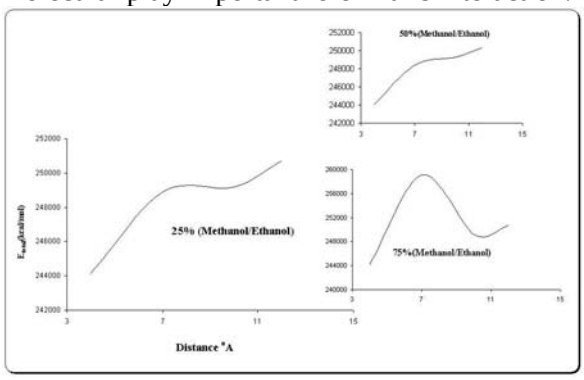

Fig.6. The total energy (kcal / mol) is calculated for interaction SnO_2 with different wt.% methanol /ethanol in distance (Å) at 343K by Monte Carlo simulation.

The results are calculated by Monte Carlo simulation that they are tabulated in tables 1-2. The efficiency of a Monte Carlo-based search engine depends on the interplay of the energy update protocol and the type of conformational movements used to modify a given conformation. The total energy and kinetic energy are approximating same in both methods with addition distance mean.

The RMS gradient gives an indication of the deviation from an optimized structure. The computations of two electron integrals and their derivatives are time-consuming, because of the huge number of the two electron integrals even for a medium size of molecule. This option applies to single point calculations only. Hyper Gauss always computes the gradients in doing geometry optimization, molecular dynamics, and vibration calculations. We choose the precision of the optimization in the Semi-empirical optimization or ab initio optimization dialog box in Hyperchem 7.0 program package. Suitable default values for ending an optimization calculation are either an RMS gradient of 0.1 kcal/mol.Å or a maximum number of cycles that

is 15 times the number of atoms involved in the calculation. In general, you must use a gradient limit. For improved precision, use a lower gradient limit.
For most organic molecules, this will result in an acceptance ratio of about 0.9, which means that about 50% of all moves are accepted. Increasing the size of the trial displacements may lead to more complete searching of configuration space, but the acceptance ratio will, in general, increase. Smaller displacements generally lead to higher acceptance ratios but result in more limited sampling. There has been little research to date on what the optimum value of the acceptance ratio should be.

A theoretical study of the adsorption and dissociation of ethanol on stoichiometric SnO_2 (110) surfaces was carried out by Calatayud et al. [13]. For one mono-layer coverage the C–O bond cleavage process was favored. This appears to be in contradiction to the experimental results discussed above where ethoxide and formaldehyde production was observed. However, oxygen vacancies were important in these experiments and defects were not taken into account in the theoretical studies.

CONCLUSION

Band bending induced by charged molecules cause the increase or decrease in surface conductivity responsible for the gas response signal.

The SnO_2 (110) shows the most complex behavior of the three surface orientations studied. Experimentally it has been found that it reduces at the lowest temperature under vacuum but a high degree of disorder observed in STM studies made it impossible to derive a reliable surface model [14].This structure was found to two research groups independently [15]. The catalytic activity of SnO_2 may be closely related to its gas sensing properties for reducing and oxidizing gases [16]. A change in the oxidation potential of the gas phase results in a shift in the surface phase diagram towards an oxygen rich or poor surface. These surface phases have different properties resulting in altered molecule–surface interactions.
The total energy depends linearly on the temperature that it increased with addition temperature so this interaction is endothermic that it was increased with addition distance mean that have indicated interaction between SnO_2 (110) and different wt.% methanol/ethanol molecules in low distance.
The diffusion behavior can be clearly distinguished as either normal-mode or single file mode in time scales of about 1000 ps. It is possible to show that setting a threshold of 1 on the movement of the dihedrals of the them backbone in a single Monte Carlo step, the mean quantities associated with the off-equilibrium dynamics are well reproduced, while the good description of higher moments requires smaller moves.

REFERENCES

1. H.L. Hartnagel, A.L. Dawar, A.K. Jain, C. Jagadish, Semiconducting Transparent Thin Films, Institute of Physics Publishing, Bristol and Philadelphia, 1995.
2. See, for example, Cunningham, D. A. H. Vogel, W. Kageyama, H. Tsubota, S. Haruta, M. J. Catal. 1 (1998) 177. (b) Vartuli, J. C. Schmitt, K. D. Kresge, C. T. Roth, W. J. Leonowicz, M. E. McCullen, S. B. Hellring, S. D. Beck, J. S. Schlenker, J. L. Olson, D. H. Sheppard, E. W. Chem. Mater. 6 (1994) 2317-2326. (c) Janicke, M. T. Landry, C. C. Christiansen, S. C. Kumar, D. Stucky, G. D. hmelka, B. F. J. Am. Chem. Soc.120 (1998) 6940.
3. P. T. Moseley, Solid State Gas Sensors (Review Article); Meas. Sci. Technol. 8 (1997) 223.
4. Paraguay-Delgado, F. Antunez-Flores, W. Miki-Yoshida, M. Aguilar-Elguezabal, A.Santiago, P. Diaz, R and Ascencio, J. A. Microsc Microanal 10 (2004)(Suppl 2), 340.
5. Opel, W. G¨. Schierbaum, K.D. Sens. Actuators. B: Chem. 26/27 (1995) 1.
6. M. Batzill, U. Diebold, The surface and materials science of tin oxide. Progress in Surface Science 79 (2005) 47.
7. P.A. Cox, R.G. Egdell, W.R. Flavell, R. Helbig, Observation of surface optical phonons on SnO_2 (110), Vacuum 33 (1983) 835.
8. Hyperchem 7.0, Hypecube Inc., Gainesville, FL, USA, 2001.

9. N. Metropolis, A.W. Rosenbluth, M.N. Rosenbluth, A.H. Teller, E. Teller, Equation of state calculations by fast computing machines, J. Chem. Phys. 21 (1953) 1087.
10. N. Strecker, V. Moroz, M. Jaraiz, Proceedings of the 2002 International Conference on Computational Nanoscience, 2002; p. 247.
11. M. P. Allen, D.J. Tildesley, Computer Simulation of Liquids, Oxford University Press, New York .1987; p.18.
12. G. Tiana, L. Sutto, R.A. Broglia, Physica A: Statistical Mechanics and its Applications. 380 (2007) 241.
13. M. Calatayud, J. Andre's, A. Beltra'n, A theoretical analysis of adsorption and dissociation of CH_3OH on the stoichiometric SnO_2 (110) surface, Surf. Sci. 430 (1999) 213.
14. M. Batzill, K. Katsiev, U. Diebold, Surface morphologies of SnO_2 (110), Surf. Sci. 529 (2003) 295.
15. W. Bergermayer, I. Tanaka, Reduced SnO_2 surfaces by first-principles calculations, Appl. Phys. Lett. 84(2004) 909.
16. Kocemba, S. Szafran, J. Rynkowski, T. Paryjczak, Relationship between the catalytic and detection properties of SnO_2 and Pt/SnO_2 systems, Ads. Sci. Technol. 20 (2002) 897.